

# DEVELOPMENT OF THE TECHNOLOGY FOR OBTAINING PLGA AND DIPROPOXYBACTERIOPURPURINIMIDE-BASED NANOPARTICLES. EVALUATION OF PHYSICO-CHEMICAL AND BIOLOGICAL PROPERTIES OF THE OBTAINED DELIVERY SYSTEM

Sapelnikov M.D.<sup>1</sup>, Nikolskaya E.D.<sup>2</sup>, Morozova N.B.<sup>3</sup>, Plotnikova E.A.<sup>3</sup>,  
 Efremenko A.V.<sup>4,5</sup>, Panov A.V.<sup>1,6</sup>, Grin M.A.<sup>1</sup>, Yakubovskaya R.I.<sup>3</sup>

<sup>1</sup>Federal State Budget Educational Institution of Higher Education "MIREA – Moscow Technological University", Moscow, Russia

<sup>2</sup>Russian research center for molecular diagnostics and therapy (RCMDT), Moscow, Russia

<sup>3</sup>P.A. Herzen Moscow Oncology Research Center – branch of FSBI NMRRC of the Ministry of Health of Russia, Moscow, Russia

<sup>4</sup>Shemyakin & Ovchinnikov Institute of Bioorganic Chemistry of the Russian Academy of Sciences, Moscow, Russia

<sup>5</sup>Lomonosov Moscow State University, Moscow, Russia

<sup>6</sup>ZAO "Institute of pharmaceutical technologies", Moscow, Russia

## Abstract

The article describes the process of developing a technology for producing nanoparticles based on a copolymer of lactic and glycolic acids (PLGA) containing dipropoxybacteriopurpurinimide (DPBPI) for photodynamic therapy of malignant tumors of various origins. Technological parameters for optimizing the method in order to obtain nanoparticles with specified characteristics are presented in this paper. As a result, the nanoparticles sample with an average particle diameter of  $222.6 \pm 2.8$  nm;  $\xi$ -potential  $26.3 \pm 4.61$  mV; polydispersity index 0.144; the total content of DPBPI in PLGA-DPBPI nanoparticles 13.6% were obtained. In accordance with the developed technique, the batch of PLGA-DPBPI nanoparticles was developed for further biological studies. In vitro experiments on A549 human non-small cell lung carcinoma for DPBPI, delivered as a part of PLGA-DPBPI nanoparticles, and an EL cremophor-based emulsion (CrEL-DPBPI) showed a similar intracellular distribution (concentrated in vesicular cell structures and diffusely distributed in cytoplasm), as well as high photo induced activity and the absence of dark cytotoxicity in case of PLGA-DPBPI nanoparticles. The study of the PLGA-DPBPI nanoparticles specific activity in vivo on the S37 mouse soft tissue sarcoma model showed the selective accumulation of DPBPI in tumor tissue and the almost complete elimination of DPBPI from the body within 48 hours, as well as significant antitumor efficacy in PDT.

**Keywords:** photodynamic therapy, nanoparticles, PLGA, photosensitizer, photoinduced activity, photoinduced antitumor efficacy, dipropoxybacteriopurpurinimide.

**For citations:** Sapelnikov M.D., Nikolskaya E.D., Morozova N.B., Plotnikova E.A., Efremenko A.V., Panov A.V., Grin M.A., Yakubovskaya R.I. Development of the technology for obtaining PLGA and dipropoxybacteriopurpurinimide-based nanoparticles. Evaluation of physicochemical and biological properties of the obtained delivery system, *Biomedical Photonics*, 2019, vol. 8, no. 1, pp. 4–17. (in Russian) doi: 10.24931/2413–9432–2019–8–1–4–17.

**Contacts:** Sapelnikov M.D., e-mail: maxsapelnikov@gmail.com

## РАЗРАБОТКА ТЕХНОЛОГИИ ПОЛУЧЕНИЯ НАНОЧАСТИЦ НА ОСНОВЕ PLGA И ДИПРОПОКСИБАКТЕРИОПУРПУРИНИМИДА. ОЦЕНКА ФИЗИКО-ХИМИЧЕСКИХ И БИОЛОГИЧЕСКИХ СВОЙСТВ ПОЛУЧЕННОЙ СИСТЕМЫ ДОСТАВКИ

М.Д. Сапельников<sup>1</sup>, Е.Д. Никольская<sup>2</sup>, Н.Б. Морозова<sup>3</sup>, Е.А. Плотникова<sup>3</sup>,  
 А.В. Ефременко<sup>4,5</sup>, А.В. Панов<sup>1,6</sup>, М.А. Грин<sup>1</sup>, Р.И. Якубовская<sup>3</sup>

<sup>1</sup>МИРЭА – Российский технологический университет, Москва, Россия

<sup>2</sup>Всероссийский научный центр молекулярной диагностики и лечения (ВНЦМДЛ), Москва, Россия

<sup>3</sup>МНИОИ им. П.А. Герцена – филиал ФГБУ «НМИЦ радиологии» Минздрава России, Москва, Россия

<sup>4</sup>Институт биоорганической химии им. академиков М. М. Шемякина и Ю. А. Овчинникова Российской академии наук, Москва, Россия

<sup>5</sup>МГУ им. М.В. Ломоносова, Москва, Россия

<sup>6</sup>ЗАО «Институт фармацевтических технологий», Москва, Россия

## Резюме

В статье описан процесс разработки технологии получения наночастиц на основе сополимера молочной и гликолевой кислот (PLGA), включающих дипропоксибacteriopurpurинимид (DPBPI) и предназначенных для фотодинамической терапии (ФДТ) злокачественных новообразований различного генеза. В работе подобраны технологические параметры, позволяющие оптимизировать метод получения наночастиц с заданными характеристиками, в результате был получен образец сферических частиц, обладающая средним диаметром частиц  $222,6 \pm 2,8$  нм;  $\xi$ -потенциалом  $-26,3 \pm 4,61$  мВ; индексом полидисперсности 0,144; общее содержание DPBPI в частицах PLGA-DPBPI составило 13,6%. В соответствии с разработанной методикой была осуществлена наработка партии наночастиц PLGA-DPBPI для дальнейших биологических исследований. В экспериментах *in vitro* на клетках немелкоклеточной карциномы легкого человека A549 для DPBPI, доставленного в клетки с помощью наночастиц PLGA-DPBPI, и эмульсии на основе кремофора EL (CrEL-DPBPI) было показано сходное внутриклеточное распределение (концентрирование в везикулярных клеточных структурах и диффузное распределение в цитоплазме), а также была показана высокая фотоиндуцированная активность и отсутствие темновой цитотоксичности в случае использования частиц PLGA-DPBPI. Изучение специфической активности наночастиц PLGA-DPBPI *in vivo* на модели саркомы мягких тканей мыши S37 показало селективное накопление DPBPI в опухолевой ткани и практически полное выведение DPBPI из организма в течение 48 ч, а также выраженную противоопухолевую эффективность при ФДТ.

**Ключевые слова:** фотодинамическая терапия, наночастицы, PLGA, фотосенсибилизатор, фотоиндуцированная активность, фотоиндуцированная противоопухолевая эффективность, дипропоксибacteriopurpurинимид.

**Для цитирования:** Сапельников М.Д., Никольская Е.Д., Морозова Н.Б., Плотникова Е.А., Ефременко А.В., Панов А.В., Грин М.А., Якубовская Р.И. Разработка технологии получения наночастиц на основе PLGA и дипропоксибacteriopurpurинимида. Оценка физико-химических и биологических свойств полученной системы доставки // Biomedical Photonics – 2019. – Т. 8, № 1. – С. 4–17. doi: 10.24931/2413-9432-2019-8-1-4-17.

**Контакты:** Сапельников М.Д., e-mail: maxsapelnikov@gmail.com

## Introduction

Today, one of the topical areas of research is the development and production of new dosage forms (DF) of hydrophobic substances with high pharmacological activity. One of the promising DFs used for these purposes is nanoparticles based on biodegradable copolymers of lactic and glycolic acids (PLGA). This form makes it possible to influence the processes of drugs delivery and deposition in the target organs and tissues [1, 2]. Particles with an average diameter of about 200 nm both effectively accumulate in organs and tissues with malignant tumors and are internalized by tumor cells [1]. The use of PLGA with a terminal carboxyl group and a 50:50 ratio of monomer units allows to obtain particles with a smaller diameter compared to other ratios of lactic and glycolic acid monomers, this effect is due to its physicochemical properties [3].

One of the groups of new compounds in which the use of the above DF is relevant is photosensitizers (PS) used for photodynamic therapy (PDT) of oncological diseases. Of particular interest are bacteriochlorins with

their intense absorption in the near IR region of the spectrum, since their therapeutic absorption window (750–850 nm) expands the possibilities for diagnosing and treating malignant neoplasms by penetrating into tissues to a depth of 20–25 mm and makes it possible to apply the currently used methods for the treatment of larger and/or deeper tumors.

For most bacteriochlorins, common shortcomings can be identified that limit their use in clinical practice [2]:

- low solubility in water, which leads to the limitation of the dose administered;
- insufficient level of selectivity and accumulation of drugs in tumor tissues and, as a consequence, a decrease in the efficiency of PDT;
- short circulation time and low level of PS accumulation in target organs and target tissues.

Thus, when obtaining new forms for this group of substances, it is important to take into account the above disadvantages and to select the optimal delivery system

to overcome them and increase the effectiveness of the PDT method.

The idea of therapeutic use of PLGA-based nanoparticles containing dipropoxybacteriopurpurinimide (DPBPI) implies selective delivery and time-controlled release of the photoactive substance into the tumor tissue, thereby reducing the non-specific toxicity of the drug, as well as its antitumor efficacy. In addition, this DF can be stored for a long period of time and can be quickly and easily produced in its consumer form.

## Materials and methods

### The development of technology for producing PLGA-DPBPI nanoparticles

#### Materials used

The DPBPI sample used for the research was produced at the Department of Chemistry and Technology of Biologically Active Compounds, Medical and Organic Chemistry named after N.A. Preobrazhensky at the Russian University of Technology. The structural formula of DPBPI is shown in Fig. 1. The concentration of DPBPI in nanoparticle samples and cremophor-based emulsions was determined spectrophotometrically at the long-wavelength absorption maximum ( $\lambda = 802$  nm) with the use of a molar extinction coefficient of 30,000 l/(mol·cm) [4].

#### Method for producing PLGA-DPBPI nanoparticles

3.0 mg of DPBPI and 50.0 mg of PLGA-COOH were dissolved in 2.0 ml of methylene chloride (viscosity: 0.17 dl/g in hexafluoroisopropanol, LACTEL® (Absorbable Polymers,

USA)) with magnetic stirring for 15 minutes. The resulting solution was added dropwise to 10.0 ml of a 1% aqueous solution of polyvinyl alcohol (PVA) in a 150 ml Drexel bottle and stirred with Variomag Multipoint magnetic stirrer (Variomag, USA) at a speed of 1120 rpm with a 9\*32 mm magnet for 10 min, with the stopper closed. Then the emulsion was subjected to treatment with an IKA Ultra Turrax T25 homogenizer (IKA, Germany) (25,000 rpm, 3 times for 1 min at 1 min intervals). The organic solvent was removed from the resulting emulsion on a rotary evaporator (LABOROTA 4000-EFFICIENT (Heidolph, Germany)) at a vacuum of 0.9–1.0 kgf/m<sup>2</sup> and a water bath temperature of 35°C until the complete removal of the organic solvent. Then the suspension was centrifuged at 14000 rpm for 30 min at +4°C in order to separate the excess amount of PVA. The supernatant liquid was decanted, and the precipitate containing the nanoparticles was suspended in 2 ml of distilled water. The sediment in the form of a suspension was subjected to ultrasonication (Transsonic T420 (Transonic, USA)) for 1 min, then the cryoprotectant was added (D-mannitol, 5.0 mg) and lyophilised for 24 h, with subsequent freezing in a freezer (-20°C) and freezer unit (-70°C). The obtained particles were stored at +4°C in a place without exposure to light.

In accordance with this method, PLGA-DPBPI nanoparticles were produced for further biological studies.

#### The determination of dimensions and $\xi$ -potential of PLGA-DPBPI nanoparticles

The particle size was determined by dynamic light scattering, and  $\xi$ -potential was found by electrophoretic

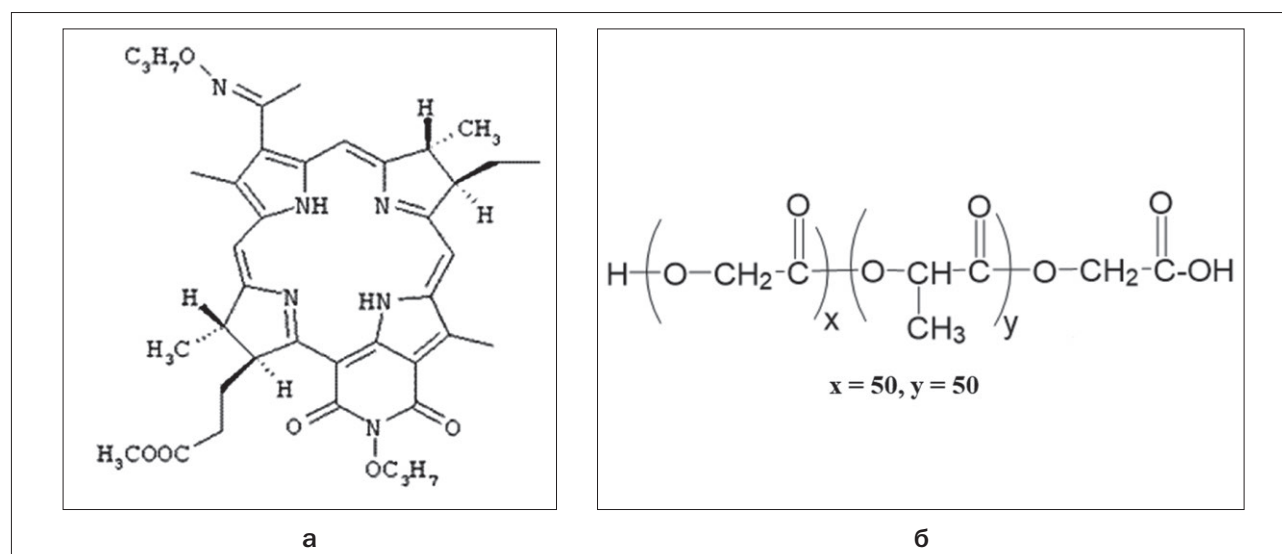


**Рис. 1.** Химические структуры:

- а. Дипропоксибактериопурпуринимид (DPBPI);  
 б. Соплимер молочной и гликолевой кислот (PLGA-COOH 50/50)

**Fig. 1.** The chemical structures of:

- а. Dipropoxybacteriopurpurinimide (DPBPI);  
 б. Copolymer of lactic and glycolic acids (PLGA-COOH 50/50)

method. The tested sample of PLGA-DPBPI nanoparticles was used to prepare an aqueous suspension with a concentration of 1 mg/ml. The measurements were performed with Zetasizer Nano ZS ZEN 3600 analyzer (Malvern Instruments, UK) under a standardized protocol (SOP).

*The determination of water content in the lyophilisate of PLGA-DPBPI nanoparticles with K. Fisher method (semi-micromethod)*

A test sample of the PLGA-DPBPI nanoparticles lyophilisate in an amount of 20.0 to 100.0 mg (exact sample weight) is placed in a titrator vessel (Metrohm 852 KF Titrando, Switzerland), and 5.0 ml of methyl alcohol is added. Titration is performed with a titrating solution (Fisher's reagent). Fisher's reagent is a solution of sulfur dioxide, iodine and pyridine in methanol. The instrument automatically sets the time of 10 seconds for the dissolving (or suspending) of the sample. Water content is determined with due account for the titer values. At least two parallel measurements were taken. The end of the titration was determined potentiometrically. The water content  $X$  (%) was calculated by formula 1:

$$X = [(a - b) \times T \times 100] / c, \quad (1)$$

where  $a$  is the volume of Fisher reagent consumed for titration in the main experiment, ml;  $b$  is the amount of Fisher reagent consumed for titration in the control experiment, ml;  $c$  the weight of the nanoparticles, g;  $T$  - Fisher reagent titer, g/ml.

*The determination of total DPBPI content and its degree of incorporation into PLGA-DPBPI nanoparticles by a spectrophotometric method*

A precise sample weight (4.0 mg) of the PLGA-DPBPI nanoparticle lyophilisate was dissolved in 5 ml of chloroform. The Helios  $\alpha$  spectrophotometer (Thermo Electron, USA) was used to record the electronic absorption spectra of the solution obtained in the wavelength range of 200–1000 nm. The concentration of DPBPI was determined from the values of the absorption intensity of the solution at a wavelength of 802 nm. The calculation of the total DPBPI content in a sample of nanoparticles ( $m_{DPBPI}$ , mg) was carried out as follows.

According to formula 2, the molar concentration of DPBPI (in mol/l) in chloroform solution was calculated:

$$C_m = D_{802} / K, \quad (2)$$

where  $D_{802}$  is the optical density of the sample solution at a wavelength of 802 nm,  $K$  is the molar extinction coefficient of the substance, equal to 30,000 l/(mol · cm).

Then, taking into account the known molecular mass of DPBPI (696.84 g/mol), the mass concentration of DPBPI (in g/l) in the resulting solution was calculated under formula 3:

$$C = C_m \times M_{DPBPI}, \quad (3)$$

where  $C_m$  is the molar concentration of the substance in the solution, mol/l;  $M_{DPBPI}$  is the molar mass of the substance, g/mol.

With formula 4, the mass of DPBPI (mg) in chloroform solution was calculated.

$$m_{DPBPI} = C \times V, \quad (4)$$

where  $C$  is the mass concentration of the substance, mg/ml;  $V$  is the volume of chloroform solution, ml.

The total content of DPBPI ( $W_{DPBPI}$ , mg / g) in the resulting batch of particles ( $m_{NP}$ , mg) was determined by formula 5.

$$W_{DPBPI} = (m_{DPBPI} / m_{NP}) \times 1000, \quad (5)$$

where  $m_{DPBPI}$  is the mass of DPBPI in a solution of chloroform, mg,  $m_{NP}$  is the mass of the studied sample of PLGA-DPBPI nanoparticles, mg.

The number of included DPBPI or the degree of its inclusion ( $S$ , wt. %) in the nanoparticles was determined by formula 6.

$$S = (m_{DPBPI} / m_{loaded}) \times 100\%, \quad (6)$$

where  $m_{DPBPI}$  is the mass of DPBPI in chloroform solution,  $m_{loaded}$  is the mass of DPBPI initially loaded to produce nanoparticles.

*The analysis of the morphology of PLGA-DPBPI nanoparticles by scanning electron microscopy*

The tested sample of PLGA-DPBPI nanoparticles was used to prepare an aqueous suspension with a concentration of 1 mg/ml, which was applied with a microdosing device onto a double-sided adhesive carbon tape. It was left to dry for about 20 minutes. Images of the samples were obtained with JSM-7401F transmission electron microscope (JEOL, Japan).

*The analysis of the morphology of PLGA-DPBPI nanoparticles by transmission electron microscopy*

To carry out this analysis, 5–10  $\mu$ l of an aqueous suspension of the studied samples of nanoparticles with a concentration of 1 mg/ml were applied onto freshly ionized carbon-form films, after 2 min the excess liquid was removed with filter paper and the preparations were contrasted with 1% aqueous uranyl acetate solution. The preparations were analyzed with an electron microscope (JEOL 100CX, Japan) at an accelerating voltage of 80 kV. The negatives (magnification of 20,000–50,000 times) were scanned with a resolution of 1200 dpi (dots per inch).

### **In vitro studies**

#### *Materials used*

The biological model used for *in vitro* experiments was non-small cell lung human carcinoma cells of the



A549 human line. Cell cultivation was performed in DMEM medium (PanEco, Russia) with the addition of 10% fetal bovine serum (Hyclone, Thermo Fisher Scientific, USA) and 2 mM glutamine (PanEco, Russia) at 37°C in 5% CO<sub>2</sub> atmosphere, hereinafter referred to as the complete medium. The cells were re-seeded twice a week. The viability of the cells used in the experiments was at least 95%.

#### *Sample preparation for in vitro experiments*

The nanoparticles loaded with DPBPI (PLGA-DPBPI) were suspended in 50 mM Na-phosphate buffer (pH 7.4) to achieve a concentration of 0.3 mM for the active substance, thus obtaining a suspension (test sample). The positive control was produced by trituration of dry DPBPI powder in polyethoxylated castor oil, Cremophor EL (CrEL), with further ultrasound treatment in a sonication bath for 20 minutes and subsequent dilution with 50 mM Na-phosphate buffer (pH 7.4) to 10% CrEL. DPBPI concentration in the composition of Cremophor EL emulsion (CrEL-DPBPI) was 0.6 mM. In the experiments, a freshly prepared suspension of PLGA-DPBPI and an emulsion of CrEL-DPBPI were used.

#### *The study of the accumulation of PLGA-DPBPI in cells of human non-small cell lung carcinoma A549*

To assess the intracellular internalization of PLGA-DPBPI and CrEL-DPBPI, cells of the A549 line, upon reaching the logarithmic growth phase, were seeded on coverslips in 24-well plates (concentration  $7.5 \times 10^4$  cells/well) and incubated for 24 hours at + 37°C 5% atmosphere of CO<sub>2</sub> to achieve confluency of 70%. The cells were incubated for 2 h with the test sample and positive control at concentrations of 4 and 8 μM. The intracellular distribution (visualized by DPBPI fluorescence) was studied with LSM710META laser scanning confocal microscope (LSCM) (Zeiss, Germany). All confocal fluorescent images were obtained with an oil-immersion x63 lens (C-Apochromat, numerical aperture 1.46). The lateral resolution was 0.3 μm, and the axial resolution was 1.5 μm. The fluorescence of the samples was excited with a helium-neon laser (543 nm). For fluorescence registration, APD detection with a long-wavelength barrier filter with a 655 nm limit was used. The resulting images were processed with ImageJ application.

#### *The study of photo-induced cytotoxicity of PLGA-DPBPI in vitro*

To study the photoinduced cytotoxicity of the PLGA-DPBPI sample, A549 cells were seeded into 96-well flat-bottom plates (seeding density was  $2.0 \cdot 10^4$ ,  $1.2 \cdot 10^4$  and  $0.7 \cdot 10^4$  cells/well). The studied samples were introduced into the wells after 24 h with a range of concentrations of samples from 14.0 μM to 0.010 μM, obtained by two-fold dilution. The dark cytotoxicity of PLGADPBPI particles

was evaluated 72 hours after the sample was introduced to A549 cells with the density of  $0.7 \cdot 10^4$  cells/well. For CrEL-DPBPI, the assessment of dark cytotoxicity was carried out in a similar way after 5 and 8 hours.

Photoinduced cytotoxicity of the samples at different A549 cell seeding densities was evaluated after incubating the cells with the samples in complete medium in the tested concentration ranges for 2 h, followed by irradiation for 15 min with a 500 W halogen lamp through a 5 cm water filter and a broadband filter (the transmittance was 680–1000 nm, the light dose was 13.5 J/cm<sup>2</sup>).

To evaluate the photoinduced cytotoxicity of the samples under study as dependant on the light irradiation dose, cells with a density of  $0.7 \cdot 10^4$  cells/well were incubated with the samples in complete medium for 2 h, then they were washed three times with DMEM medium without serum, fresh complete medium was added to the cells, and they were irradiated with a 500 W halogen lamp through a 5 cm thick water filter and a broadband filter (transmission 680–1000 nm) for 15 (13.5 J/cm<sup>2</sup>), 30 (27.0 J/cm<sup>2</sup>) or 45 (40.5 J/cm<sup>2</sup>) minutes.

After irradiation, cells were incubated under standard conditions for 3 hours, and then stained with Hoechst 33342 (Sigma-Aldrich, USA) and propidium iodide (PI) (Sigma-Aldrich, USA). Hoechst 33342 (4 μM) and PI (6 μM) were added to the cells 15 minutes before the completion of incubation. The result of photodynamic exposure was analyzed with epi-fluorescence microscopy with the use of an Axio Observer fluorescence microscope (Zeiss, Germany). Stained cells were placed in a tablet on an object table of an inverted microscope and fluorescent images of Hoechst 33342 luminescence ( $\lambda_{exc}$  359–371 nm,  $\lambda_{reg} > 397$  nm) and PI ( $\lambda_{exc}$  530–585 nm,  $\lambda_{reg} > 615$  nm) in cells were recorded with the use of a digital camera. The resulting images were processed in ImageJ application, and the total number of cells and the number of dead cells were obtained for each sample. In each sample, 300–400 cells were subjected to calculation. According to the measurement results, a graph of the dependence of the percentage of surviving cells versus sample concentration was plotted. For the comparison of the photoinduced cytotoxicity of the samples, LC<sub>50</sub> and LC<sub>90</sub> values were calculated, which corresponded to the concentrations of PLGA-DPBPI and CrEL-DPBPI, by active substance, at which 50% and 90% cell death is observed, respectively.

#### *In vivo studies*

##### *Materials used*

For *in vivo* experiments, the first generation (F1) hybrid mice were used (CBA x C57Bl/6J), females (7–9 weeks old, body weight: 18–22 g) supplied by Andreevka laboratory animals breeding center of FSBRI NTsBMT of FMBA of Russia. The animals were kept in separate rooms, under controlled environmental conditions. For

the experiments, mice were inoculated with tumor cells of mouse soft tissue sarcoma, S37 line, with  $1 \cdot 10^6$  cells subcutaneously in the region of the sural muscle on the outer side of the thigh. Strain S37 was maintained in ascites form in male mice of the ICR (CD-1) line. Studies were performed on day 7 after tumor inoculation, when its volume reached 130–160 mm<sup>3</sup>.

All manipulations were carried out in accordance with national and international rules on humane treatment of animals [5, 6].

#### *Sample preparation for in vivo experiments*

To assess the distribution of PS in nanoparticles in organs and tissues of mice, as well as to study photo-induced antitumor activity, a PLGA-DPBPI sample with an active substance content of 13.6 mg/g was used. To obtain a consumer form, a weighted sample was added to a 0.9% sodium chloride solution to produce a stable pink suspension.

#### *Assessment of the distribution of PLGA-DPBPI in animal tissues and organs*

A study of the biodistribution of DPBPI, which is part of PLGA-DPBPI nanoparticles (7.5 mg/kg dose by DPBPI, intravenous administration), was carried out ex vivo in mice with developed tumor with the use of local fluorescence spectroscopy. Fluorescence was recorded by contact method on LESA laser spectral analyzer for fluorescent diagnosis of tumors (OOO "Biospec", Russia).

The objects of study were tumor tissue, skin and muscle, liver, kidneys, spleen, omentum and blood obtained from three animals for each observation interval (0.25, 2, 4, 24, and 48 hours). When fluorescence was excited in the red region of the spectrum (632.8 nm), the integrated fluorescence intensity in the spectral range of measurements (640–900 nm) was normalized by the integrated intensity of the back diffuse scattering of exciting laser radiation signal in the tissue, determining the normalized fluorescence (FN) in the tissues. The accumulation of PLGA-DPBPI in tissues was assessed by the maximum values of FN at a wavelength corresponding to the maximum fluorescence of DPBPI. During the study, the fluorescent contrast (FC) was calculated as the ratio of PN in the tumor to PN in the skin.

#### *The study of the efficiency of photodynamic therapy with the use of PLGA-DPBPI nanoparticles*

Photodynamic therapy was performed remotely on the seventh day of tumor growth of S37 sarcoma in mice with injected PLGA-DPBPI particles at a dose of 2.5 mg/kg with the active component of DPBPI. The control animals were injected isotonic 0.9% sodium chloride solution intravenously. Droperidol (solution for injections, 2.5 mg/ml, FSUE Moscow Endocrine Plant, Russia) was used as anesthesia at a dose of 0.25 mg/mouse intraperito-

neally. By the time of PDT, the volume of tumors varied from 130 to 160 mm<sup>3</sup>. For irradiation, a LED source with a wavelength of  $810 \pm 21$  nm was used (FSUE SSC NIOPIK, Russia): power density of 100 mW/cm<sup>2</sup> and energy density of 150 J/cm<sup>2</sup>. The interval between the introduction of PS and the irradiation was 2 hours. The animals that did not have continued tumor growth were observed for 90 days after treatment. The antitumor effect was evaluated according to the average values of the tumor volume, the inhibition of tumor growth, the increase in life expectancy and the recovery criterion in the control and experimental groups [7]. The tumor volume (in mm<sup>3</sup>) was calculated by formula 7,

$$V = a \times b \times c, \quad (7)$$

where  $a$  is the length,  $b$  is the width and  $c$  is the height of the tumor nodule.

#### **Statistic analysis**

The statistical processing of results was performed with Student's t-test. The construction of graphs and statistical processing was done with OriginPro 8 SRO (OriginLab Corporation, USA), Excel (Microsoft) and Statistica 8 (StatSoft) software.

## **Results and discussion**

### ***The development of technology for PLGA-DPBPI nanoparticles production and their physico-chemical properties***

Particles containing DPBPI were produced by single emulsions method [2]. As part of the development of the technology, the optimal polymer composition was determined: the concentration of surfactant and the ratio of the organic phase to the aqueous phase (O/A). The parameters of the technological process of obtaining particles and their characteristics are presented in Table 1. Within the framework of the development, technological parameters were also selected, such as the type of homogenization (with the use of an immersion homogenizer or with ultrasound (US)), the method of removing organic solvent (diffusion or vacuum), the time of centrifuging the particles suspension.

As can be seen from Table 1, an increase in PVA concentration leads to an increase in the average particle size and polydispersity index (PDI) (samples 3, 9). The reduction of PVA concentration, on the contrary, leads to the reduction of the average particle size (samples 4, 10), but results in particles with a lower content of DPBPI due to an increase in the total sample mass of PLGA-DPBPI nanoparticles, and, therefore, 1% PVA was chosen, as it made it possible to obtain particles of smaller diameter without a visible decrease in the total content of the chemical. The most optimal O/W ratio is 1: 5, since a decrease in the ratio to 1: 2.5 led to a sharp increase in size and an increase in the polydispersity of the system

(sample 6), while an increase in the ratio to 1:10 (sample 5) did not contribute to a significant decrease in size, but reduced the total content of DPBPI in the particles. The use of an ultrasonic homogenizer contributed to a slight increase in particle size (sample 8), however, the degree of inclusion of the drug was much lower, and, therefore, the use of a submersible homogenizer was the most relevant. Solvent was removed from all particles with the use of vacuum, since the use of diffusion at atmospheric pressure resulted in broad size distribution peaks of the particles and the formation of a polydisperse system (sample 1). An increase in the time of particle suspension centrifuging from 15 to 30 min, in its turn, also made it possible to reduce the average particle size in a sample with a simultaneous decrease in PDI, which suggests that the optimal conditions for obtaining particles with the given characteristics have been found.

As a result, the optimal parameters of the method of obtaining particles PLGA-DPBPI (sample 7) were selected, making it possible to produce particles with improved physicochemical characteristics, such as the maximum values of the total substance content and the degree of sorption, monodisperse particle size distribution (PDI below 0.250), the average particle diameter of less than 250 nm, which was the reason for their selection for further experiments. The water content in the resulting PLGA-DPBPI nanoparticle lyophilisate (sample 7) was determined to be no more than 1.5%, and this value was taken into account in all the calculations. The total DPBPI content values obtained are given for anhydrous substance.

The particle size and their spherical shape were confirmed with the use of transmission electron microscopy and scanning electron microscopy (Fig. 2).

In this way, further experiments on the study of the efficiency of internalization of the particles obtained by

**Таблица 1**

Влияние технологических параметров на основные физико-химические характеристики полученных частиц PLGA-DPBPI

**Table 1**

The influence of technological parameters on the major physico-chemical characteristics of the obtained PLGA-DPBPI NPs

№ образца PLGA-DPBPI PLGA-DPBPI sample №	ПВС, % PVA, %	О/В O/W	Удаление растворителя Evaporation of organic solvent	Тип гомогенизатора Homogenizer type	t, мин t, min	W <sub>DPBPI</sub> мг/г W <sub>DPBPI</sub> mg/g	S, % масс. S, % w.	Средний диаметр, нм Mean diameter, nm	ξ-потенциал, мВ ξ-potential, mV	ПДИ PDI
1	1	1:5	Диффузия Diffusion	Погружной гомогенизатор Immersion homogenizer	15	9,6	28,7	485,1±2,3	-23,8±4,09	0,392
2	1	1:5			15	9,5	26,3	490,1±3,0	-24,6±2,87	0,230
3	2	1:5			15	13,4	35,1	761,3±4,5	-27,4±2,65	0,354
4	0,5	1:5			15	10,2	46,8	540,8±2,4	-20,1±3,42	0,325
5	1	1:10			15	8,1	72,6	523,2±2,2	-17,2±3,21	0,263
6	1	1:2.5			15	10,4	63,4	834,3±1,7	-14,4±2,86	0,368
7	1	1:5			30	13,6	86,1	222,6±2,8	-26,3±4,61	0,144
8	1	1:5	Вакуум Vacuum	УЗ-гомогенизатор US-homogenizer	30	16,9	36,4	261,5±3,2	-23,2±3,92	0,205
9	2	1:5		Погружной гомогенизатор Immersion homogenizer	30	15,6	25,2	340,2±2,4	-20,3±2,47	0,356
10	0.5	1:5			30	12,4	30,3	245,1±3,6	-19,2±4,06	0,232

О/В – соотношение органической фазы к водной; t – время центрифугирования

ПДИ – индекс полидисперсности

O/W – ratio of organic phase to water; t – centrifugation time

PDI – polydispersity index

tumor cells and their photodynamic activity in *in vitro* and *in vivo* models were performed with the use of PLGA-DPBPI-7.

### **Biological properties of PLGA-DPBPI. *In vitro* studies**

*Study of the accumulation of PLGA-DPBPI in A549 lung adenocarcinoma cells*

With the use of laser scanning confocal microscopy (LSCM), it was found that DPBPI in the PLGA-DPBPI particles accumulates in the cytoplasmic region of A549 cells. At the same time, DPBPI concentration is observed in vesicular cell structures of submicron size, as well as diffuse staining of the cytoplasm (Fig. 3 II). Partial co-localization of nanoparticles with lipid droplets is observed (Fig. 3 ж, з), which is characteristic of cycloimide derivatives of bacteriochlorin p [8].

Since DPBPI has hydrophobic properties, in the control group, Cremophor EL (CrEL) was chosen as a solubilizer, which is able to stabilize non-aggregated forms of tetrapyrrole compounds in aqueous solutions and is not toxic to cells *in vitro* at low concentrations [8–10]. It is important to note that CrEL is used in clinical practice [11].

By the use of LSCM method, it was discovered that the cells incubated with CrEL-DPBPI have an intracellular distribution of DPBPI similar to that of nanoparticles (Fig.3 I). Thus, the inclusion of DPBPI in the composition of nanoparticles does not block its penetration into cells and does not affect the nature of the intracellular distribution of DPBPI.

### *PLGA-DPBPI photoinduced cytotoxicity study*

In experiments on the study of the cytotoxicity of PLGA-DPBPI, it was found that the PLGADPBPI sample

did not show toxicity to A549 cells at high concentrations and long incubation times (more than 8 hours), whereas the use of DPBPI, which is part of CrEL-DPBPI (positive control), was limited by CrEL cytotoxicity. The maximum indicators for its use are no more than 5 hours with a concentration not higher than 14  $\mu\text{M}$  (Fig. 4).

In the study of photoinduced cytotoxicity, it was shown that PLGA-DPBPI particles cause concentration-dependent death of A549 cells (Fig. 5). At different cell seeding densities ( $0.7 \cdot 10^4$  cells/well;  $2 \cdot 10^4$  cells/well, Fig. 5a), the ratio of the parameters  $\text{LC}_{50}$  and  $\text{LC}_{90}$  (the concentrations causing the death of 50% and 90% of the cells, Table 2) of PLGA-DPBPI to CrELDPBPI remains the same, at  $1.6 \pm 0.1$  (Table.3). An increase in the light dose leads to an increase in the photodynamic activity of both forms of DPBPI (Fig. 5, Table. 2). The washing of A549 cells after 2 hours of incubation with PLGA-DPBPI or CrEL-DPBPI before irradiation did not lead to a decrease in the photodynamic effect (Fig. 5b). Consequently, photoinduced cell death occurs due to the activation of the intracellular concentration of PLGA-DPBPI or the positive control (Fig. 5, Table 2). The photodynamic effect of PLGA-DPBPI can be limited by the rate of intracellular release of the active substance from nanoparticles, and, therefore, the photoinduced cytotoxicity of compounds was studied at different irradiation times. The samples were preliminarily removed from the cell medium (the cells were washed after 2 h of incubation with the samples). An increase in the irradiation time and, consequently, the light dose of irradiation led to an increase in the photodynamic effect for both PLGA-DPBPI and CrEL-DPBPI (Fig. 5b, Table 2). The ratio of  $\text{LC}_{50}$  and  $\text{LC}_{90}$  parameters of PLGA-DPBPI to CrEL-DPBPI varies within the range of  $1.6 \div 2.4$  (table 3).

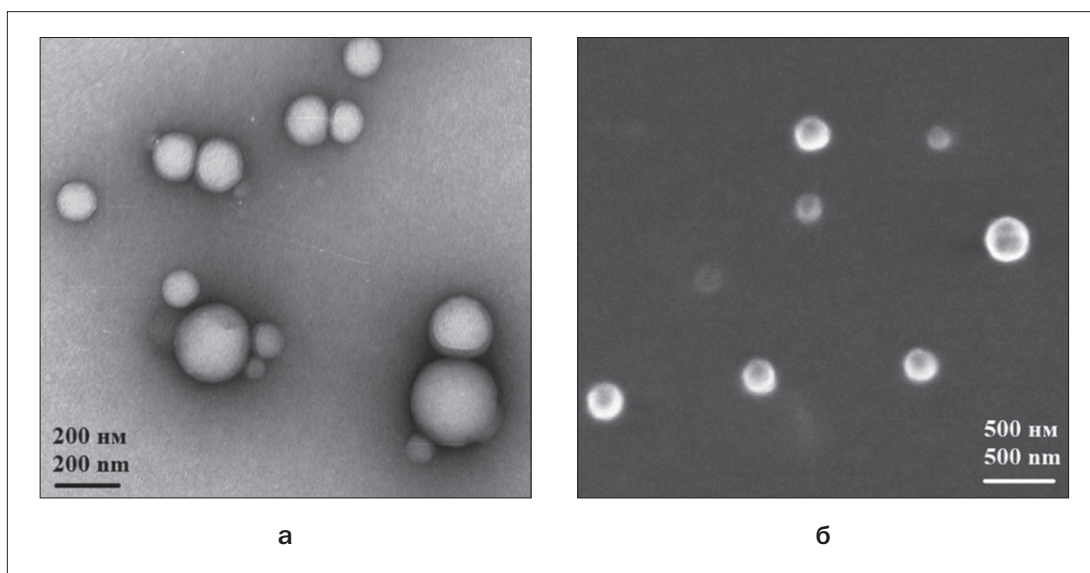


**Рис. 2.** Микрофотографии частиц PLGA-DPBPI, полученных методом просвечивающей электронной микроскопии (а) и сканирующей электронной микроскопии (б)

**Fig. 2.** TEM (a) and SEM (б) microphotographs of PLGA-DPBPI NPs



At the same time, a twofold increase in the dose (and a twofold increase in the exposure time) resulted in the decrease in  $LC_{50}$  by 2.53 times for positive control and 1.75 times for PLGA-DPBPI. A further x1.5 increase in dose (irradiation time) reduced the  $LC_{50}$  by a factor of 1.49 for a positive control, whereas in the sample under study the  $LC_{50}$  value decreased by a factor of 1.7.

Thus, the use of DPBPI in the composition of PLGA-DPBPI nanoparticles contributes to the accumulation of DPBPI in the cytoplasm of A549 tumor cells and causes photo-induced cytotoxicity, which is confirmed by the preservation of the photodynamic properties of DPBPI after its inclusion into the composition of the polymeric form.

With increasing exposure time and light dose, the photo-induced cytotoxicity of PLGA-DPBPI increases linearly, whereas CrELDPBPI tends to decrease.

### Biological properties of PLGA-DPBPI. In vivo studies

#### Distribution of PLGA-DPBPI in animal tissues and organs

The analysis of the fluorescence spectra obtained ex vivo after intravenous administration of DPBPI to mice showed that the maximum fluorescence for the dye in

the organs and tissues of animals was recorded at  $817 \pm 3$  nm.

The studied PLGA-DPBPI nanoparticle preparation, when administered intravenously, entered the tumor tissue S37 relatively quickly, with the FN level reaching a maximum value 2 hours after the injection, at the level of  $7.1 \pm 1.1$  relative units (table 4). After 48 h, the mean FN level in the tumor was 9.8% of the maximum recorded value.

In normal skin, the maximum accumulation of DPBPI was determined in the time interval from 0.25 to 2 h after intravenous administration of the dye (the FN value was  $2.6 \pm 0.3$  -  $3.5 \pm 0.3$  relative units), and after 24 hours DPBPI was no longer determined. The maximum value of FC relative to the skin was recorded in the time interval from 2 to 4 h after the dye injection and amounted to 2.7–3.0 relative units.

Therefore, with PDT, irradiation has to be performed 2 hours after the introduction of PLGA-DPBPI nanoparticles, when the accumulation in the tumor and the fluorescent contrast reach their maximum value.

DPBPI was determined in the bloodstream within 24 hours after its administration. Low values of normalized fluorescence ( $4.3 \pm 0.4$  relative units and  $4.8 \pm 0.6$  relative

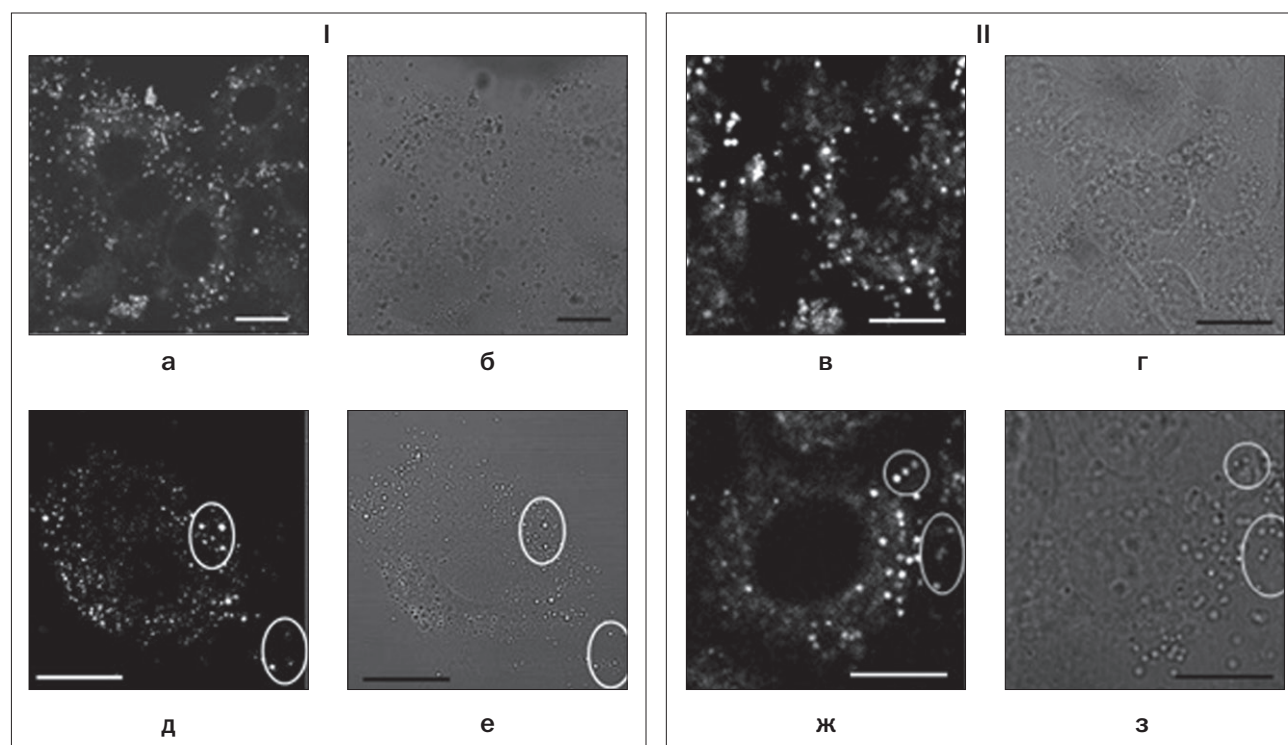


**Рис. 3.** Типичное внутриклеточное распределение DPBPI, входящего в состав CrEL-DPBPI (I) и PLGA-DPBPI (II), в клетках немелкоклеточной карциномы легкого человека линии A549, полученные методом ЛСКМ (а, в, д, ж) и в проходящем белом свете (б, г, е, з) после инкубации клеток с образцами в концентрации 4 мкМ в течение 2-х ч. На изображениях д-з показана со-локализация DPBPI с липидными каплями (области обведены овалами). Масштаб соответствует 15 мкм

**Fig. 3.** Typical intracellular distribution of DPBPI in CrEL-DPBPI (I) and PLGA-DPBPI (II) complexes inside A549 human non-small lung cancer cells. Images were obtained by LSCM (a, в, д, ж) and in transmitted white light (б, г, е, з) after incubation of cells with samples at the concentration of 4  $\mu$ m for 2 h. The co-localization of DPBPI with lipid drops (the areas are circled ovals) is shown in the images д-з. Scale bar is equal to 15  $\mu$ m

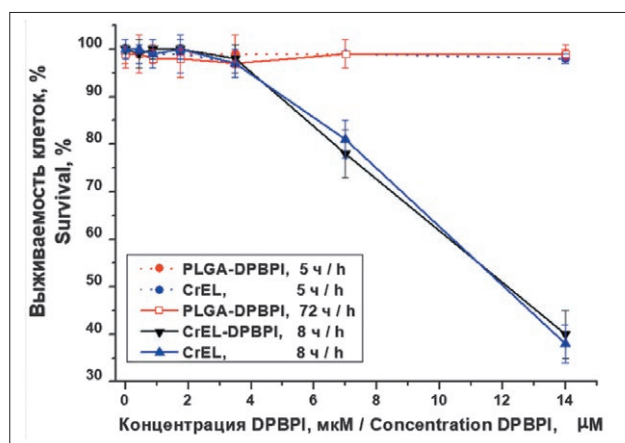


**Рис. 4.** Выживаемость клеток немелкоклеточной карциномы легкого человека линии A549 от концентрации PLGA-DPBPI, CrEL-DPBPI и CrEL при различном времени инкубации при изучении темновой цитотоксичности

**Fig. 4.** Survival of non-small cell lung carcinoma cells of the A549 line from the concentration of PLGA-DPBPI, CrEL-DPBPI and CrEL at different times of incubation in the study of dark cytotoxicity

units, respectively) were recorded in the muscle tissue and omentum, which decreased by 71.4% and 83.3% of the maximum recorded value, respectively. After 48 h, FN measured in the skin and in the omentum was at the background level. In the main internal organs, the maximum accumulation of DPBPI was registered in the liver and spleen 15 minutes after the administration, with FN of  $31.3 \pm 1.4$  relative units and  $25.9 \pm 1.8$  relative units, respectively. 24 hours after the intravenous administration of the dye, the level of normalized fluorescence in the liver and spleen decreased by 88.5% and 89.7% of

the maximum value, respectively, and after 48 hours only background values were observed. In the kidneys, the maximum values of the normalized fluorescence of DPBPI were recorded 2 h after injection ( $12.0 \pm 0.2$  relative units), and after 48 h the kidney fluorescence was found to be at the background level. The data obtained indicate rapid elimination of the photosensitizer from the body of mice and the predominant removal of the chemical through the excretory system of the liver.

#### *Photo-induced antitumor activity of PLGA-DPBPI in mice with S37 sarcoma*

Upon the performance of PDT with PLGA-DPBPI, the irradiated animals with S37 sarcoma developed an edema within 2 hours, which persisted for 4 days. No lethality of animals from phototoxic shock after a PDT session was observed.

The data presented in Fig. 6 and 7 show that the photosensitizer has an antitumor effect. With the use of PLGA-DPBPI at a dose of 2.5 mg/kg (by active substance) and a two hour interval between irradiation and administration, the average tumor volume in the experimental group increased slowly relative to the tumor volume in the control group, the tumor growth inhibition (TGI) on day 22 after the PDT session being 71%. The maximum TGI value was 78% on day 11. For 90 days, 33% of the mice did not demonstrate continued tumor growth.

Thus, the effect of PDT on the S37 transplanted tumor with the use of PLGA-DPBPI made it possible to achieve a pronounced antitumor effect in this experiment (life expectancy increase: 83%, recovery coefficient: 33%).

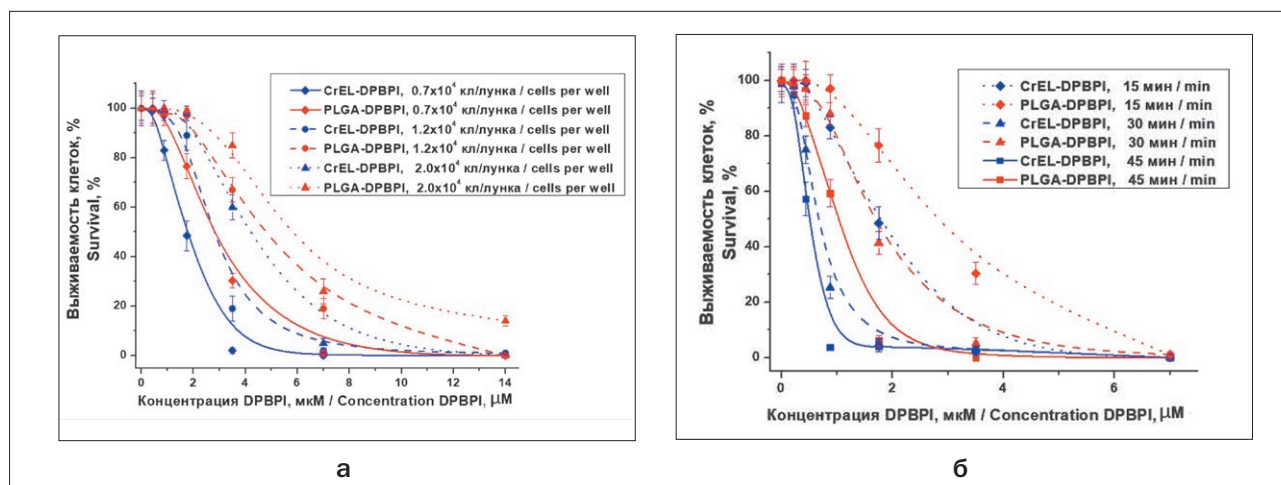


**Рис. 5.** Выживаемость клеток немелкоклеточной карциномы легкого человека линии A549 от концентрации CrEL-DPBPI и PLGA-DPBPI при изучении фотоиндуцированной цитотоксичности, где (а) – после 2 ч инкубации и облучения галогенной лампой в течение 15 мин ( $13.5 \text{ Дж/см}^2$ ) при различной плотности клеток; (б) – после 2 ч инкубации, отмывки клеток от соединений во внешней среде и облучения галогенной лампой в течение различного времени облучения. Плотность клеток  $0.7 \cdot 10^4$  кл./лунка

**Fig. 5.** Survival of non-small cell lung carcinoma cells of the A549 line from the concentration of CrEL-DPBPI and PLGA-DPBPI in the study of photoinduced cytotoxicity. (a) – after 2 hours of incubation and irradiation with a halogen lamp for 15 minutes ( $13.5 \text{ J/cm}^2$ ) at different cell densities; (б) – after 2 hours of incubation, washing cells from compounds in the environment and irradiation with a halogen lamp for various irradiation times. The density of cells was  $0.7 \cdot 10^4$  cells/well

**Таблица 2**

Значения  $LC_{90}$  и  $LC_{50}$  для CrEL-DPBPI и PLGA-DPBPI при различной концентрации клеток (облучение галогенной лампой в течение 15 мин, 13,5 Дж/см<sup>2</sup>) и времени облучения (плотность клеток 0,7·10<sup>4</sup> кл/лунка, с проведением отмывки)

**Table 2**

The values of  $LC_{90}$  and  $LC_{50}$  for CrEL-DPBPI and PLGA-DPBPI at various cells concentrations (halogen lamp exposure for 15 minutes (13.5 J/cm<sup>2</sup>)) and irradiation time (cell density of 0.7·10<sup>4</sup> cells / well, with washing)

Концентрация клеток, кл/лунка Cells concentration, cells/well	$LC_{90}$ , мкМ $LC_{90}$ , μM		$LC_{50}$ , мкМ $LC_{50}$ , μM	
	PLGA-DPBPI	CrEL-DPBPI	PLGA-DPBPI	CrEL-DPBPI
0,7·10 <sup>4</sup>	4,7±0,1	2,9±0,1	2,8±0,1	1,7±0,1
1,2·10 <sup>4</sup>	8,0±0,1	3,9±0,1	4,7±0,1	2,8±0,1
2·10 <sup>4</sup>	8,5±0,1	5,3±0,1	5,6±0,1	3,7±0,1
Время облучения, мин (световая доза, Дж/см <sup>2</sup> ) Exposure time, min (light dose, J/cm <sup>2</sup> )	$LC_{90}$ , мкМ $LC_{90}$ , μM		$LC_{50}$ , мкМ $LC_{50}$ , μM	
	PLGA-DPBPI	CrEL-DPBPI	PLGA-DPBPI	CrEL-DPBPI
15 (13,5)	4,7±0,1	2,9±0,1	2,8±0,1	1,7±0,1
30 (27)	2,5±0,1	1,1±0,05	1,6±0,1	0,67±0,05
45 (40,5)	1,6±0,1	0,67±0,05	0,96±0,05	0,45±0,03

**Таблица 3**

Отношения  $(LC_{90})_2/(LC_{90})_1$  и  $(LC_{50})_2/(LC_{50})_1$  для CrEL-DPBPI (1) и PLGA-DPBPI (2) при различной концентрации клеток (облучение галогенной лампой в течение 15 мин (13,5 Дж/см<sup>2</sup>)) и времени облучения (плотность клеток 0,7·10<sup>4</sup> кл/лунка, с проведением отмывки)

**Table 3**

$(LC_{90})_2/(LC_{90})_1$  and  $(LC_{50})_2/(LC_{50})_1$  rates for CrEL-DPBPI (1) and PLGA-DPBPI (2) at various cell concentrations (halogen lamp exposure for 15 minutes (13.5 J/cm<sup>2</sup>)) and irradiation time (cell density of 0.7·10<sup>4</sup> cells / well, with washing)

Концентрация клеток, кл/лунка Cells concentration, cells/well	$(LC_{90})_2/(LC_{90})_1$	$(LC_{50})_2/(LC_{50})_1$
0,7·10 <sup>4</sup>	1,62	1,65
1,2·10 <sup>4</sup>	2,05	1,68
2,0·10 <sup>4</sup>	1,60	1,51
Время облучения, мин (световая доза, Дж/см <sup>2</sup> ) Exposure time, min (light dose, J/cm <sup>2</sup> )	$(LC_{90})_2/(LC_{90})_1$	$(LC_{50})_2/(LC_{50})_1$
15 (13,5)	1,62	1,65
30 (27)	2,27	2,39
45 (40,5)	2,39	2,13

\*(1) – CrEL-DPBPI; (2) – PLGA-DPBPI

**Таблица 4**

Интенсивность нормированной флуоресценции DPBPI в органах и тканях мышей с саркомой S37 после введения наночастиц PLGA-DPBPI в дозе 7,5 мг/кг

**Table 4**

The intensity of the normalized fluorescence of DPBPI in organs and tissues of mice with S37 sarcoma after administration of PLGA-DPBPI polymer particles at a dose of 7.5 mg / kg

Органы и ткани Organs and tissues	Контроль* (Фон) Control* (Background)	Нормированная флуоресценция (ФН), отн. ед. Normalized fluorescence (FN), rel. units				
		Сроки измерения нормированной флуоресценции после введения образца, ч The timing of the measurement of normalized fluorescence after the introduction of the sample, h				
		0,25	2	4	24	48
Опухоль Tumor	3,0±0,2	4,5±0,4	7,1±1,1	5,4±0,7	3,9±0,1	3,4±0,1
Кожа Skin	1,5±0,1	3,5±0,3	2,6±0,3	1,8±0,2	1,6±0,1	1,6±0,1
Мышца Muscle	2,7±0,1	4,1±0,5	4,3±0,4	3,9±0,3	3,1±0,4	2,8±0,1
Сальник Adipose tissue	3,0±0,3	4,2±0,2	4,8±0,6	3,2±0,2	3,2±0,2	3,1±0,1
Печень Liver	7,8±0,2	31,2±1,4	23,4±1,0	18,3±0,1	10,5±0,3	8,6±0,6
Почки Kidneys	7,6±0,2	10,8±0,2	12,0±0,2	9,8±1,2	8,3±0,1	7,8±0,2
Селезенка Spleen	9,4±0,3	25,9±1,8	20,7±1,0	17,0±0,9	11,1±0,6	10,2±0,5
Кровь Blood	4,0±0,5	22,3±0,2	7,7±0,1	6,1±0,1	4,2±0,1	3,9±0,1
ФК**	-	1,3	2,7	3,0	2,4	2,1
FC**	-	1,3	2,7	3,0	2,4	2,1

\* Контроль – мыши без воздействия (фон);

\*\* ФК (флуоресцентная контрастность) =  $\frac{FN_{\text{опухоль}}}{FN_{\text{кожа}}}$

\* Control – mice without exposure (background);

\*\* FK (fluorescent contrast) =  $\frac{FN_{\text{tumor}}}{FN_{\text{skin}}}$ , rel. units.

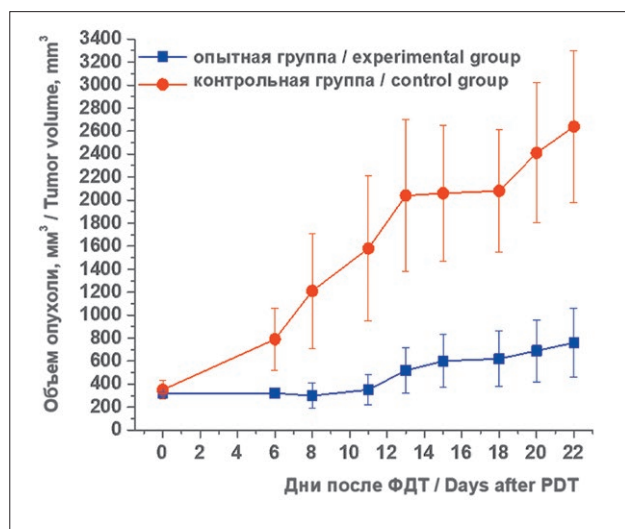


**Рис. 6.** Объем опухоли S37 у мышей после проведения ФДТ (150 Дж/см², время экспозиции 2 ч) после введения PLGA-DPBPI (в дозе 2,5 мг/кг) в контрольной и опытной группах  
**Fig. 6.** S37 tumor volume in mice after PDT (150 J/cm², exposure time 2 h) after administration of PLGA-DPBPI (at a dose of 2.5 mg/kg) in the control and experimental groups

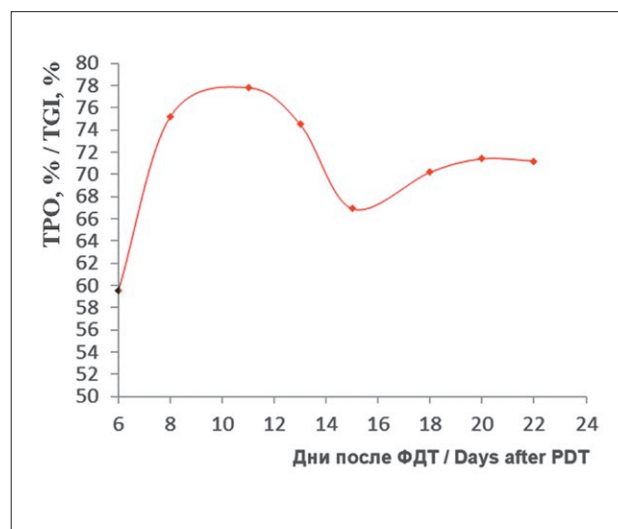


**Рис. 7.** Торможение роста опухоли (ТРО, %) на 6–22 сут после проведения ФДТ (150 Дж/см², время экспозиции 2 ч) с использованием PLGA-DPBPI (в дозе 2,5 мг/кг)  
**Fig. 7.** Inhibition of tumor growth (TGI, %) on days 6–22 after PDT (150 J/cm², exposure time 2 hours) using PLGA-DPBPI (2.5 mg/kg)



## Conclusion

The authors developed a technology for producing PLGA-based nanoparticles containing DPBPI and possessing optimal physicochemical characteristics, such as average particle size,  $\xi$ -potential value, the degree of inclusion and the substance content in particles. *In vitro* experiments recorded intracellular accumulation and distribution of DPBPI in the composition of PLGA-DPBPI particles in A549 cells, the nature of which coincided with the distribution of DPBPI in the control composition (CrEL-DPBPI). It was shown that high concentrations of the particles and long incubation times do not lead to dark cytotoxicity. The antitumor efficacy of PLGA-DPBPI particles was comparable to the effect

of CrEL-DPBPI, which is confirmed by the preservation of the photo-induced DPBPI activity after its incorporation into the polymer matrix. *In vivo* experiments showed accumulation of particles in tumor tissue with PC of up to 3.0 relative units, as well as the almost complete elimination of DPBPI from the body after 48 h. For skin, this value was 24 hours, which is important given the specific nature of the photodynamic therapy procedure. A photoinduced antitumor activity of the use of PLGA-DPBPI was also shown when performing PDT on the S37 soft tissue sarcoma model, with the cure rate of the animals reaching 33%. The data produced make it possible to conclude that the further study of PLGA-DPBPI particles may produce valuable results.

## REFERENCES

1. Rejman J., Oberle V., Zuhorn I.S., Hoekstra D. Size-dependent internalization of particles via the pathways of clathrin and caveolae-mediated endocytosis, *Biochem. J.*, 2004, no. 377, pp. 159–169.
2. Sapelnikov M.D., Panov A.V., Nikolskaya E.D., Grin M.A. Development of delivery systems for highly effective photosensitizers applicable for photodynamic therapy of cancer, *Biopharmatsevticheskiy jurnal*, 2018, vol. 10, no 1, pp. 14–25. (in Russian)
3. Nikolskaya E., Sokol M., Faustova M., Zhunina O., Mollaev M., Yabbarov N., Tereshchenko O., Popov R., Severin E. The comparative study of influence of lactic and glycolic acids copolymers type on properties of daunorubicin loaded nanoparticles and drug release, *Acta of Bioeng. and Biomech.*, 2018, vol. 20, no. 1, pp. 65–77.
4. Pantyushenko I.V., Grin M.A., Yakubovskaya R.I., Plotnikova E.A., Morozova N.B., Tsygankov A.A., Mironov A.F. A novel highly effective IR photosensitizer in the bacteriochlorophyll A series for photodynamic therapy of cancer, *Vestnik MITHT*, 2014, vol. 9, no. 3, pp. 3–10. (in Russian)
5. *Prilozhenie A k Evropeyskoy konventsii ob ohrane pozvonochnykh zhivotnykh, ispol'zuemykh dlya eksperimentov i v drugih nauchnykh tselyakh (ETS 123)* [Appendix A of the European convention for the protection of vertebrate animals used for experimental and other scientific purposes (ETS No. 123)], 13 p. Available at: <https://rm.coe.int/168007a6a8> (accessed 26.02.2019)
6. *Rukovodstvo po sodержaniyu i uhotu za laboratornymi zhivotnymi (stat'ya №5 konventsii)* [Guidelines for the maintenance and care of laboratory animals (Article 5 of the Convention)], transl. by Krasilnischikova M.S., Belozertseva I.V. Saint-Petersburg, 2014. 102 p. Available at: <http://ruslasa.ru/wp-content/uploads/2017/06/Приложение-А-к-ETS.pdf> (accessed 26.02.2019)
7. Yakubovskaya R.I., Kazachkina N.I., Karmakova T.A., et al. *Methodical recommendations on the study of photoinduced antitumor properties of drugs*. In: Guide to conducting preclinical studies of medicines. Edited by A.N. Mironov. Moscow, Grif & Ko Publ., 2012, pp. 657–71. (in Russian)
8. Feofanov A., Grichine A., Karmakova T., Plyutinskaya A., Lebedeva V., Filyasova A., Yakubovskaya R., Mironov A., Egret-Charlier M., Vigny P. Near-infrared photosensitizer based on a cycloimide derivative of chlorin p6: 13,15-N-(3'-hydroxypropyl)cycloimide chlorin p6, *Photochem. Photobiol.*, 2002, no. 75, pp. 633–643.
9. Nazarova A., Ignatova A., Feofanov A., Karmakova T., Pljutinskaya A., Mass O., Grin M., Yakubovskaya R., Mironov A., Maurizot J.-C. 13,15-N-cycloimide derivatives of chlorin p6 with isonicotinyl substituent are photosensitizers targeted to lysosomes, *Photochem. Photobiol. Sci.*, 2007, no. 6, pp. 1184–1196.

## ЛИТЕРАТУРА

1. Rejman J., Oberle V., Zuhorn I.S., Hoekstra D. Size-dependent internalization of particles via the pathways of clathrin and caveolae-mediated endocytosis // *Biochem. J.* – 2004. – No. 377. – P. 159–169.
2. Сапельников М.Д., Панов А.В., Никольская Е.Д., Грин М.А. Разработка систем доставки высокоэффективных фотосенсибилизаторов для фотодинамической терапии рака // *Биофармацевтический Журнал* – 2018. – Т. 10, № 1. – С. 14–25.
3. Nikolskaya E., Sokol M., Faustova M., et al. The comparative study of influence of lactic and glycolic acids copolymers type on properties of daunorubicin loaded nanoparticles and drug release // *Acta of Bioeng. and Biomech.* – 2018. – Vol. 20, No. 1. – P. 65–77.
4. Пантюшенко И.В., Грин М.А., Якубовская Р.И. и др. Новый высокоэффективный ИК-фотосенсибилизатор в ряду бактериохлорофилла А для фотодинамической терапии рака // *Вестник МИТХТ*. – 2014. – Т. 9, № 3. – С. 3–10.
5. Приложение А к Европейской конвенции об охране позвоночных животных, используемых для экспериментов и в других научных целях (ETS 123). – 13 с. Адрес доступа: <https://rm.coe.int/168007a6a8> (дата обращения 26.02.2019)
6. Руководство по содержанию и уходу за лабораторными животными (статья №5 конвенции) / пер. с англ. М.С. Красильниковой и И.В. Белозерцевой. – Санкт-Петербург, 2014. – 102 с. Адрес доступа: <http://ruslasa.ru/wp-content/uploads/2017/06/Приложение-А-к-ETS.pdf> (дата обращения 26.02.2019)
7. Якубовская Р.И., Казачкина Н.И., Кармакова Т.А. и др. Методические рекомендации по изучению фотоиндуцированных противоопухолевых свойств лекарственных средств // *Руководство по проведению доклинических исследований лекарственных средств*. Под ред. А.Н. Миронова и др. – М.: Гриф и К, 2012. – С. 657–71.
8. Feofanov A., Grichine A., Karmakova T., Pljutinskaya A., Lebedeva V., Filyasova A., Yakubovskaya R., Mironov A., Egret-Charlier M., Vigny P. Near-infrared photosensitizer based on a cycloimide derivative of chlorin p6: 13,15-N-(3'-hydroxypropyl)cycloimide chlorin p6 // *Photochem. Photobiol.* – 2002. – No. 75. – P. 633–643.
9. Nazarova A., Ignatova A., Feofanov A., et al. 13,15-N-cycloimide derivatives of chlorin p6 with isonicotinyl substituent are photosensitizers targeted to lysosomes // *Photochem. Photobiol. Sci.* – 2007. – No. 6. – P. 1184–1196.
10. Efremenko A.V., Ignatova A.A., Borsheva A.A., et al. Cobalt bis(dicarbollide) versus closo-dodecaborate in boronated chlorin e6 conjugates: implications for photodynamic and boron-neutron capture therapy // *Photochem. Photobiol. Sci.* – 2012. – Vol. 11, No. 4. – P. 645–652.

10. Efremenko A.V., Ignatova A.A., Borsheva A.A., Grin M.A., Bregadze V.I., Sivaev I.B., Mironov A.F., Feofanov A.V. Cobalt bis(dicarbollide) versus closo-dodecaborate in boronated chlorin e6 conjugates: implications for photodynamic and boron-neutron capture therapy, *Photochem. Photobiol. Sci.*, 2012, vol. 11, no. 4, pp. 645–652.
11. Loi S., Rischin D., Michael M., Yuen K., Stokes K.H., Ellis A.G., Millward M.J., Webster L.K. A randomized cross-over trial to determine the effect of Cremophor EL on the pharmacodynamics and pharmacokinetics of carboplatin chemotherapy // *Cancer Chemother. Pharmacol.*, 2004, vol. 54, no. 5, pp. 407–414.